

# PHASE-RESOLVING MODELING AND OBSERVATIONS OF NEARSHORE WAVE TRANSFORMATIONS IN A COMPLEX REEF ENVIRONMENT

Camilla Tognacchini, University of Hawai'i at Manoa, [camillat@hawaii.edu](mailto:camillat@hawaii.edu)  
Assaf Azouri, University of Hawai'i at Manoa, [assaf@hawaii.edu](mailto:assaf@hawaii.edu)  
Fatima-Zahra Mihami, University of Hawai'i at Manoa, [fzmihami@hawaii.edu](mailto:fzmihami@hawaii.edu)  
Ning Li, University of Hawai'i at Manoa, [ningli@hawaii.edu](mailto:ningli@hawaii.edu)  
Volker Roeber, Université de Pau et des Pays de l'Adour, [volker.roeber@univ-pau.fr](mailto:volker.roeber@univ-pau.fr)  
Martin Guiles†, University of Hawai'i at Manoa, †Deceased July 4, 2023.  
Douglas S. Luther, University of Hawai'i at Manoa, [dluther@hawaii.edu](mailto:dluther@hawaii.edu)

## INTRODUCTION

Wave-driven run-up events are severely impacting West Maui's (WM) coastline with episodic inundation and chronic shoreline erosion. A combination of background sea level, tides, and sea and swell (SS) driven components, such as swash and infragravity (IG) waves contribute to the level of run-up experienced at the shore. The setup, swash, and IG wave responses under different SS conditions are highly variable along the WM coastline due to complex nearshore fringing reef-type bathymetry and coastal geomorphology. Simulating these responses to large swell events at different locations along the WM coast is necessary for accurate estimation of local run-up, enabling forecasting of, and community preparation for, coastal inundation events. The Pacific Islands Ocean Observing System (PacIOOS) Coastal Hazards Group (CHG) has implemented a two-dimensional phase-resolving numerical nearshore wave model of weak nonlinearity and dispersion (Roeber and Cheung, 2012), using high resolution bathymetry and topography data around WM. The phase-resolving model accounts for the cross- and along-shore transformations of gravity and IG wave energy for estimation of wave run-up. In recent efforts, an improved and computationally more efficient new model version (Mihami, 2023) was implemented that allows for faster computations thus expanding the possibilities and breadth of applications over larger domains.

## METHODS

The Boussinesq-type nearshore models (Roeber and Cheung, 2012, and Mihami, 2023) are evaluated for the WM domain versus observations of seasonal energetic swell events. Nearshore sea level observations are derived from bottom water pressure records collected at different depths (1-13 meters) and locations, including two relatively compact arrays, along the WM coastline, from November 2018 - June 2020. Records of wave amplitude and direction were also collected at both arrays. The wave and sea level observations were compared with model results for different swell events at various locations along the WM coastline.

The objective is realistic numerical reproduction of the particular wave conditions that are comparable to field observations from WM. The boundary conditions of the nearshore model are high-resolution, spatially variable, hourly energy spectra from a series of numerical wind and spectral wave models (GFS; Environmental Modeling Center, 2003, WRF; Skamarock et al., 2008, WW3; Tolman, 2014, and SWAN; Booij et al., 1999)

operated at PacIOOS for the Hawaiian Islands (Figure 1).

## RESULTS

The use of realistic wave conditions and spatially varying spectra allow us to compare the in situ observations versus model results within the domain in order to understand the model's capabilities. The comparisons reveal a high degree of agreement in both the SS and IG period bands, from 8 seconds up to 10 minutes. Auto- and cross-spectral analyses are used as methods to compare and investigate the spatial variability of the nearshore wave energy.

The results show high alongshore variability in setup, swash, and IG energy; which strongly depend on the local bathymetry and coastal geomorphology. Both the model and observations reveal a high variability in IG amplitudes resulting from complex IG wave processes, see for example Figure 2. At both arrays the comparisons between observed and computed coherence phases and amplitudes (Figure 2) demonstrate that an adequately designed and depth-integrated model can well account for the frequency-dependent, spatial variability of the nearshore wave-driven phenomena that contribute to local run-up.

## FUTURE WORK

There is a growing need for accurate, spatially-variable modeling of the nearshore wave field as coastlines become increasingly vulnerable to wave run-up events due to sea level rise. Our in-house model development work (Mihami, 2023) allows us to strategically improve and expand the model's applicability towards more accurate and complete real-time predictions of hazardous nearshore wave conditions.

## REFERENCES

Booij, Ris, and Holthuijsen (1999): A third-generation wave model for coastal regions: 1. Model description and validation. *Journal of Geophysical Research: Oceans*, 104(C4), 7649-7666.

Environmental Modeling Center (2003): The GFS Atmospheric Model. NOAA/ NCEP/ Environmental Modeling Center Office Note 442, pp. 14.

Mihami (2023): Development of a phase-resolving computer model for operational nearshore wave assessment. PhD Dissertation, Université de Pau et des Pays de l'Adour.

Roeber and Cheung (2012): Boussinesq-type model for energetic breaking waves in fringing reef environments. Coastal Eng., vol. 70: pp 1-20.

Tolman (2014): User manual and system documentation of WAVEWATCH III TM version 4.18. Technical note, MMAB Contribution, 316, pp. 311.

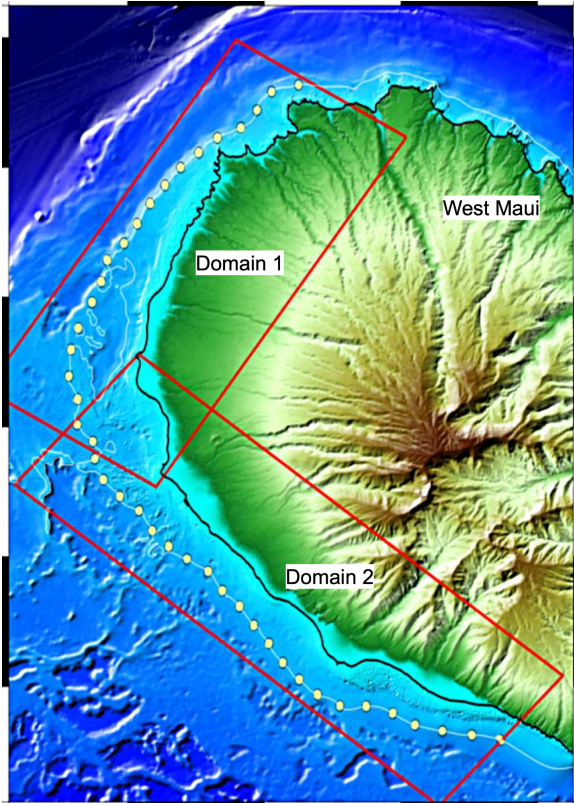


Figure 1. Map of the two-domain (red rectangles) setup for nearshore modeling of gravity wave energy transformations along the WM coastline. The spatially-variable directional wave spectra from the high-resolution SWAN are extracted at 42 virtual gauges (yellow circles in the figure, located along the 40 meter depth contour of each of the model domains) and then employed by the wavemakers at the domain boundaries.

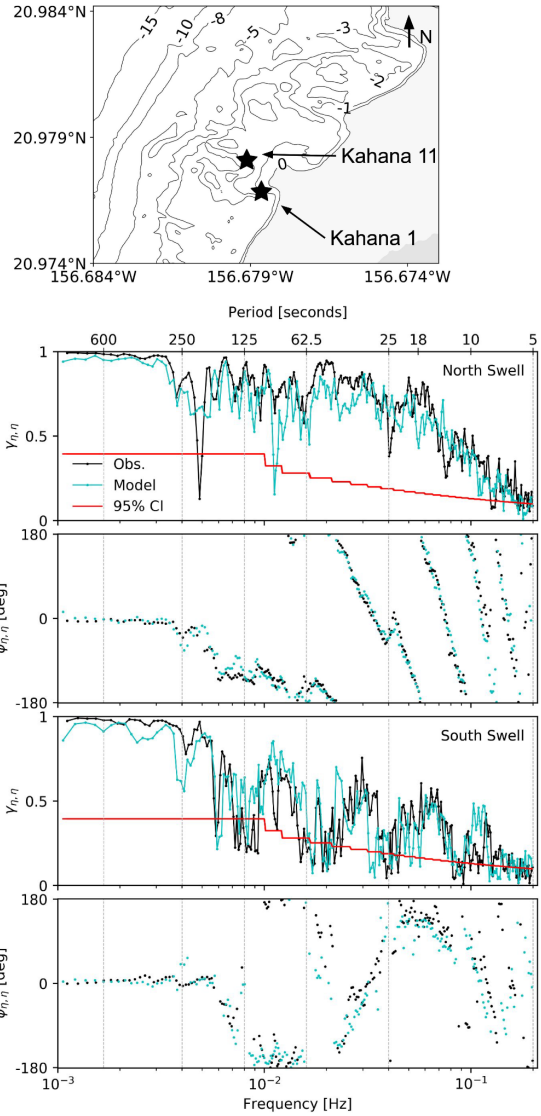


Figure 2. Coherence amplitude and phase of sea level model simulations (Model) and observations (Obs.) from stations Kahana 11 and Kahana 1, located 100 meters apart. The plots are produced from five two-hour long segments of data. Top two panels: North swell event on December 7, 2019. Bottom two panels: South swell event on July 14, 2019. The 95% level of confidence (95% CI) for the coherence amplitude is plotted in red.